Journal of Optoelectronics and Advanced Materials Vol. 7, No. 2, April 2005, p. 1091 - 1101

# LIDAR CALIBRATED SATELLITE SENSED PRIMARY PRODUCTION IN THE SOUTHERN OCEAN

R. Barbini, F. Colao, R. Fantoni, L. Fiorani[*], I. G. Okladnikov[a], A. Palucci

ENEA, FIS-LAS, Via Fermi 45, 00044 Frascati, Italy
[a]ENEA guest (IMCES, SCERT, Akademicheskii Avenue 10/3, 634055 Tomsk, Russia)

The carbon cycle is among the more important global phenomena affecting the Earth's climate. The Southern Ocean is probably one of the less studied oceanic provinces and a thorough understanding of its role in that natural process requires further study. In this paper, new estimates of the primary production (PP) of Antarctic waters from 1997 to 2003 are provided. They are based on a PP model tuned in Antarctica and on satellite derived chlorophyll-a (Chl-a) concentrations calculated with an original bio-optical algorithm calibrated with lidar measurements carried out in the Southern Ocean. The results presented here indicate that usual PP models applied to standard Chl-a concentrations can underestimate PP up to 50%.

(Received February 4, 2005; accepted March 23, 2005)

*Keywords*: Remote sensing, Lidar, Satellite radiometer, Chlorophyll, Primary productivity

## 1. Introduction

The biogeochemical cycles taking place in the world's ocean are very important for the future development of the Earth's climate [1]. For this reason, a large series of passive and active remote sensors aimed to the sea observation has been developed in the last decades. In particular, ocean colour radiometers [2] and lidar fluorosensors [3] have been employed extensively. Such systems differ by operating principle and typical carrier: while the first ones are passive sensors aboard satellites, the second ones are are active sensors aboard ships. This explains why they are in some sense complementary: from one hand, ocean colour satellite radiometers provide global coverage but need atmospheric corrections [4] and calibrations/validations [5] of the bio-optical algorithms [6], both involving in situ measurements, from the other hand, lidar fluorosensors do not depend on the atmospheric column or the water type but are limited in space by the ship track and in time by the cruise duration.

The calibration/validation problem is particularly crucial for the Southern Ocean that, despite its important role in controlling the climate, is less represented than other oceanic regions in the data sets used to calibrate the bio-optical algorithms of the satellite radiometers [5]. A further problem is introduced in Antarctica by a series of circumpolar fronts that define different oceanographic provinces where the development of endemic phytoplankton is favoured [7].

Laser remote sensing activities began at the ENEA (Italian Agency for New Technologies, Energy and the Environment) research centre of Frascati in the eighties [8]. Since 1997, ELF (ENEA Lidar Fluorosensor) participated to oceanographic campaigns in Antarctica aboard the research vessel (RV) *Italica* [9]. In 2000, comparative studies of ELF and the ocean colour satellite radiometer SeaWiFS (Sea-viewing Wide Field-of-view Sensor) [10] started [11]. In this study, a regional calibration of the SeaWiFS chlorophyll-a (Chl-a) algorithm has been carried out in the Southern Ocean and, as a result, new primary production (PP) estimates from 1997 to 2003 have been calculated.

[*]Corresponding author: fiorani@frascati.enea.it

## 2. Instruments and methods

ELF and SeaWiFS have already been described by Barbini et al. [9] and Hooker et al. [10], respectively: here we will only recall their main characteristics. ELF is based on laser-induced fluorescence (LIF) and continuously provides concentrations of chromophoric dissolved organic matter (CDOM) and phytoplankton pigments all along the ship track. SeaWiFS is an ocean colour scanning radiometer: it derives Chl-a from radiance measurements at different wavelengths.

### 2.1. Bio-optical algorithm

In the following we focus on the data fusion between ELF measurements and SeaWiFS products. Usual match up analysis of satellite versus in situ Chl-a values relies in relatively few stations were seawater samples are analysed with high performance liquid chromatography (HPLC). For example, the Chl-a comparison between satellite retrievals and in situ data from the fourth SeaWiFS reprocessing is based on 262 match ups [12]. On the contrary, many lidar measurements can be compared with one satellite retrieval: ELF emits a laser pulse every 0.1 s and as a result acquires thousands of signals during the time taken by the ship to span a SeaWiFS pixel. Moreover, while a station cover only one point of a pixel, ELF data represent a wider zone because they are distributed along a track crossing the pixel.

Another interest of the present study is its geographical location: most of the experimental points used up to now to calibrate the bio-optical algorithms were not taken in polar regions [5]. This could explain the observation of underestimations of PP in the Southern Ocean [13].
As a case study we consider the 16$^{th}$ Italian Antarctic Oceanographic Campaign (January 5$^{th}$ 2001 – February 26$^{th}$ 2001) and we define (Fig. 1):

- the Ross Sea Region (RSR) as the area delimited by the coast and a line (straight in the cylindrical equidistant projection) from a point near Cape Adare (72° S, 170° E) to a point near Cape Colbeck (76° S, 158° W),
- the Ross Sea Sector (RSS) as the zone of Southern Ocean from the coast of Antarctica north to 50° S latitude in the 160° E – 130° W sector.

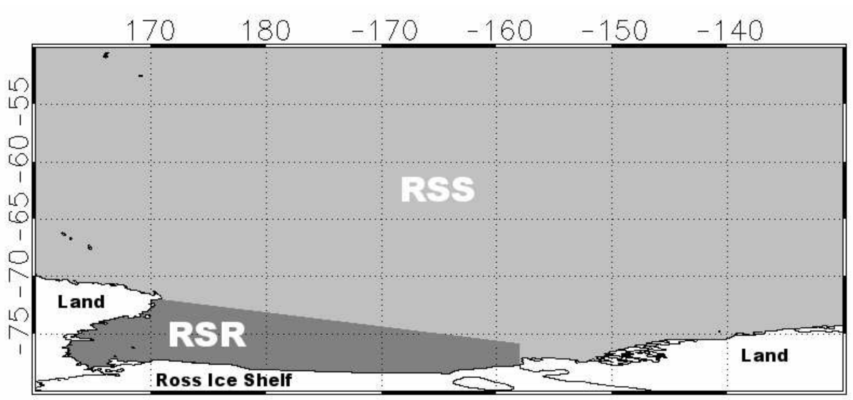


Fig. 1. Zones of interest: Ross Sea Region, in dark grey and Ross Sea Sector, in dark and light grey.

Although RSR does not coincide exactly with the Ross Sea, its simple definition was a necessary compromise: the calculation of the bio-optical properties in RSR, rather than in the Ross Sea, saves computing time because the satellite products are usually delivered in the cylindrical equidistant projection and it is fast to determine whether a pixel is above or below a straight line. The rationale in the demarcation of RSS is to allow one to compare the present study to that of Arrigo et al. [13].

L3 SeaWiFS products were considered here: although this choice involved a rather poor granularity (about 9 km × 9 km), it ensured the highest accuracy and has been judged as the best compromise. The granularity of ELF is different, since the laser footprint on the water surface sizes around 0.1 m. In order to better associate lidar and radiometer data, all the ELF measurements falling in a SeaWiFS pixel were averaged, thus representing a track of length ~ 10 km and width: ~ 0.1 m.

The SeaWiFS Chl-a bio-optical algorithms [6] calculate the concentration of that pigment from the remote sensing reflectance measured by that radiometer at 490 and 555 nm. In this study, the OC1 algorithm has been tuned with the ELF data, as in a previous study [11].
OC1 [6] is expressed by

$$C = 10^{\,a_0 + a_1 \rho}\,, \tag{1}$$

where C is the Chl-a concentration in mg $m^{-3}$, $a_0$ and $a_1$ are the algorithm parameters and

$$\rho = log_{10} \frac{R_{490}}{R_{555}}\,, \tag{2}$$

where $R_\lambda$ is the remote sensing reflectance at the wavelength $\lambda$ [nm] and $\rho$ is called band ratio.

As far as temporal resolution is concerned, it would be desirable to use SeaWiFS daily products for that calibration, so that the time difference of the lidar and radiometer data is less than 24 hours. Nevertheless, if daily products are used, the concurrent measurements are too few. The 8-day products seem the best compromise: concurrent measurements are quite abundant while abrupt changes during a week are fairly rare in phytoplankton distribution. On the contrary, although monthly products would have allow one to gather even more concurrent measurements, during a month the Chl-a variation can be wide enough. Moreover, 8-day products are preferable also because the statistical error of the fitted parameters of the OC1 algorithm is lower for 8-day products than for daily or monthly products.

Although the ELF – SeaWiFS agreement is usually good, it is advisable to discard some data before calculating $a_0$ and $a_1$, e.g. cutting all the concurrent measurements with a ratio between ELF and SeaWiFS Chl-a larger than x or smaller than 1/x [11]. The appropriate value of the cut parameter x can be identified looking at the effects of that cut on the percent of discarded data and the statistical error of the fitted parameters.
Observing that:

- the percent of discarded measurement is acceptable (less than 10%) for $x \geq 4$,
- the statistical error of $a_0$ is minimum for x = 4 (although it is nearly constant for $x \geq 3$),
- the statistical error of $a_1$ is nearly constant for $x \geq 3$,

we chose x = 4, also in continuity of the value adopted for the 13th Italian Antarctic Oceanographic Campaign [11].

Table 1. Results of the ELF calibration of the SeaWiFS Chl-a bio-optical algorithm.

| Zone | Number of concurrent measurements | $a_0$ | $\sigma(a_0)$ | $a_1$ | $\sigma(a_1)$ |
|---|---|---|---|---|---|
| RSR | 1345 | 0.3713 | 0.0055 | -1.422 | 0.024 |
| RSS | 1523 | 0.3674 | 0.0059 | -1.482 | 0.023 |

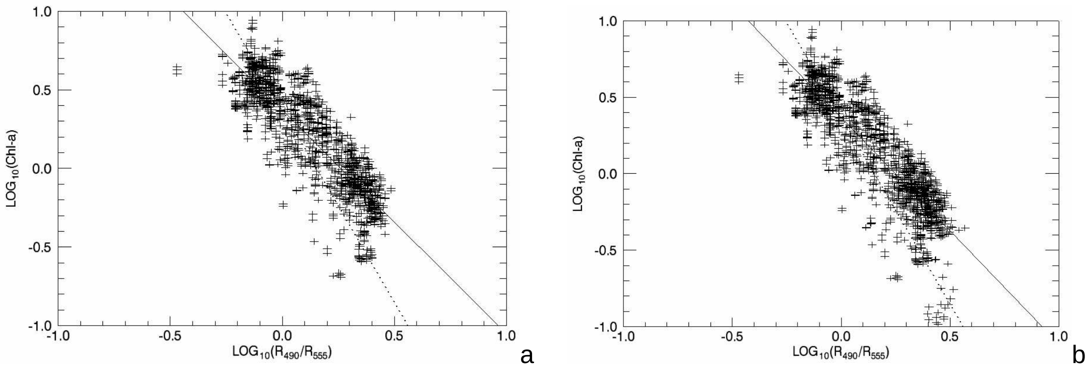


Fig. 2. ELF calibration of the SeaWiFS Chl-a bio-optical algorithm (continuous line) in: a) RSR; b) RSS. The dashed line represents the standard OC1 bio-optical algorithm.

The results of the ELF calibration of the SeaWiFS Chl-a bio-optical algorithm are summarized in table 1 and the fits are shown in Fig. 2. Let us note that only few points (178) come from RSS outside RSR: in our opinion, the calibration should be regarded as more reliable in RSR. Nevertheless, the two values of $a_0$ and $a_1$ for RSR and RSS differ less than 1 and 2 σ (standard deviation), respectively. As far as the discrepancy between the ELF-calibrated and the standard OC1 SeaWiFS Chl-a bio-optical algorithms is concerned, $a_0$ is similar but $a_1$ is rather different: in fact, in standard OC1 $a_0 = 0.3734$ and $a_1 = -2.4529$ [6]. In other words, our results indicate that in RSR standard OC1 weakly overestimate high concentrations and strongly underestimate low concentrations, confirming the findings of the 13th Italian Antarctic Oceanographic Campaign [11]. This behaviour could be linked to the bio-optical characteristics of Antarctic phytoplankton: in fact, if the northern latitudes are included (Fig. 2b) some points near the standard OC1 line are added and one could imagine that using almost only in situ measurements coming from temperate regions – as in usual SeaWiFS calibrations – one would obtain results similar to those of standard OC1.

The difference between the bio-optical algorithms calibrated with the data of 13th and 16th Italian Antarctic Oceanographic Campaigns is smaller than the statistical fluctuation: in the following we use the algorithm calibrated with the data of the 16th Italian Antarctic Oceanographic Campaign because it is based on more experimental points.

### 2.2. PP model

A large spectrum of PP models have been formulated up to now [14]. Here we will refer only to depth-integrated models and, in particular, to two widespread global models:

- a log-linear fit by Falkowski et al. [15] (called F-model in the following),
- the Vertically Generalized Production Model (VGPM) by Behrenfeld and Falkowski [14, 16] (called BF-model in the following),

and to two models optimized in Antarctica:

- the first by Dierssen et al. [17] is based on a log-linear fit (called L-model in the following),
- the second by Smith et al. [18] is VGPM calibrated in Antarctic coastal waters (called D-model in the following).

The variables used in the above mentioned models are:

- $C_{surf}$: surface chlorophyll concentration [mgChl m$^{-3}$], corresponds to the Chl-a concentration measured by ELF and SeaWiFS,
- $Z_{eu}$: euphotic zone [m], i.e. the penetration depth of 1% surface irradiance,
- $P^B_{opt}$: maximum chlorophyll-specific carbon fixation rate [mgC mgChl$^{-1}$ h$^{-1}$], observed within a water column and measured under conditions of variable irradiance during incubations typically spanning several hours,
- D: daylength [h], also called photoperiod,

- F: relative fraction of potential photosynthesis lost within the euphotic zone due to light limitation [unitless], to first order equal to the average production of the water column divided by $P^B_{opt}$,
- $PP_{eu}$: daily PP within the euphotic zone per unit of surface [mgC $m^{-2}$ $d^{-1}$].

#### *2.2.1. F-model*

The F-model is very simple and consists in the following equation

$$PP_{eu} = 621\, C_{surf}^{\;0.559}. \tag{3}$$

#### *2.2.2. BF-model*

The BF-model is probably the today reference model. It can be summarized in the following equations

$$PP_{eu} = P^B{}_{opt}\; F\; Z_{eu}\; C_{surf}\; D\,, \tag{4}$$

$$\begin{aligned} P^B{}_{opt} = & -3.27\times10^{-8}\,\mathrm{T}^7 + 3.4132\times10^{-6}\,\mathrm{T}^6 - 1.348\times10^{-4}\,\mathrm{T}^5 + \\ & + 2.462\times10^{-3}\,\mathrm{T}^4 - 0.0205\,\mathrm{T}^3 + 0.0617\,\mathrm{T}^2 + 0.2749\,\mathrm{T} + 1.2956 \end{aligned}, \tag{5}$$

$$F = 0.55. \tag{6}$$

where T is the Sea Surface Temperature (SST) in °C.

The euphotic zone can be calculated according to the relationships [19]

$$Z_{eu} = \begin{cases} 568.2\, C_{tot}^{\;-0.746} & \text{if } Z_{eu} < 102\ \mathrm{m} \\ 200.0\, C_{tot}^{\;-0.293} & \text{if } Z_{eu} \geq 102\ \mathrm{m} \end{cases}, \tag{7}$$

where

$$C_{tot} = \begin{cases} 38.0\, C_{surf}^{\;0.425} & \text{if } C_{surf} < 1\ \mathrm{mgChl\ m^{-3}} \\ 40.2\, C_{surf}^{\;0.507} & \text{if } C_{surf} \geq 1\ \mathrm{mgChl\ m^{-3}} \end{cases}. \tag{8}$$

For the daylength we used the formulas by Sellers [20].
During the 16th Italian Antarctic Oceanographic Campaign, SST in RSR is around 0 °C, as indicated by the data of the satellite sensor Advanced Very High Resolution Radiometer (AVHRR) [21] and confirmed by the measurements performed from the RV *Italica*, therefore we will assume simply

$$P^B{}_{opt} = 1.2956. \tag{9}$$

#### *2.2.3. L-model*

The L-model consists of a log-linear regression between PP and Chl-a concentration carried out in Antarctic waters:

$$PP_{eu} = 513\, C_{surf}^{\;0.725}. \tag{10}$$

#### *2.2.4. D-model*

The D-model is defined by Equation (4) and the following relationships

$$P^B{}_{opt} = 1.09\,, \tag{11}$$

$$F = 0.64\,, \tag{12}$$

$$Z_{eu} = 48.8\, C_{surf}{}^{-0.36}\,. \tag{13}$$

For the daylength we used once more the formulas by Sellers [20].

Actually, F could also be obtained with the following relationship [17]

$$F = \frac{PAR}{PAR + 11.77}\,, \tag{14}$$

where PAR is the photosynthetically available radiation. Substituting in Equation (14) the average PAR measured by ELF during the 16$^{th}$ Italian Antarctic Oceanographic Campaign we obtain

$$F = 0.652\,. \tag{15}$$

When using Equation (15) instead of Equation (12), the model will be called D'-model.

## 3. Results and discussion

The above mentioned models have been applied to RSR during the 16$^{th}$ Italian Antarctic Oceanographic Campaign, i.e. to the Chl-a concentration calculated with the ELF-calibrated SeaWiFS Chl-a bio-optical algorithm used with the related reflectance daily products of January and February 2001 (Fig. 3).

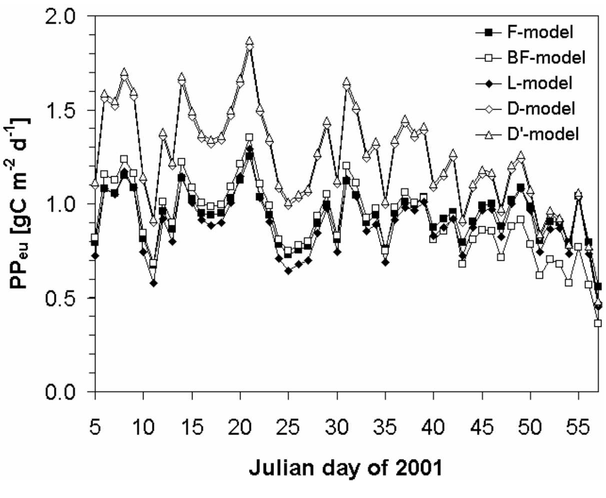


Fig. 3. Average PP calculated with the ELF-calibrated SeaWiFS Chl-a bio-optical algorithm and different PP models in RSR during the 16$^{th}$ Italian Antarctic Oceanographic Campaign.

Two classes of values can be distinguished: higher (D- and D'- models) and lower (F-, BF- and L- models). Of course, the discrepancy between D- and D'-model is small because it depends only on the little difference in the values of the F parameter. Note the effect of daylength reduction in the BF-, D- and D'-models, i.e. the models that take into account that variable (the daylength becomes smaller than 24 hours around the Julian day 40 at the 76° S latitude, i.e. in the middle of RSR).

In principle, in the Southern Ocean, Antarctic PP models should be more reliable than global PP models. Among the Antarctic PP models, the D'-model is the more attractive because it is more refined than the L-model, with respect to D-model it has been corrected with PAR measurements and agrees with other authors [13] that already suggested that PP has been underestimated in the Southern Ocean. For such reasons, in the following we will use the D'-model to provide new PP calculations.

First of all, we used the D'-model to compare PP in RSR and RSS (Fig. 4). Estimates in RSS should be taken cautiously: from one hand, as we already pointed out, the ELF calibration should be regarded as more reliable in RSR, from the other hand, the D'-model has been tuned in coastal zones. Nevertheless, it is confirmed that the PP is lower in RSS than RSR. Moreover, as one can expect, the values of the two zones are well correlated.

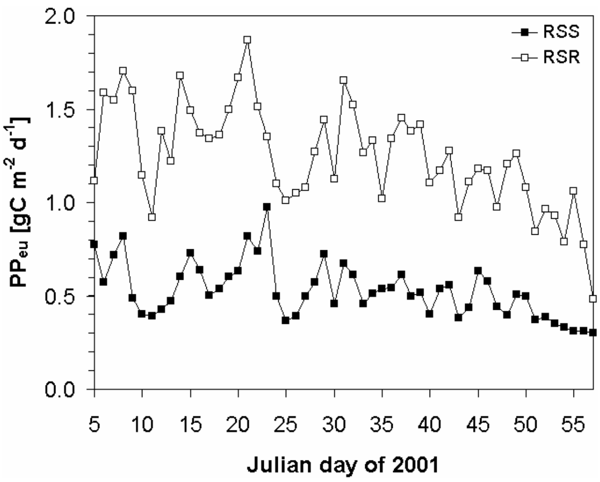


Fig. 4. Average PP calculated with the ELF-calibrated SeaWiFS Chl-a bio-optical algorithm and the D'- model in RSR and RSS during the 16th Italian Antarctic Oceanographic Campaign.

The temporal averaging of PP in RSR and RSS during the 16th Italian Antarctic Oceanographic Campaign (Table 2) points out that the usual estimates should be reviewed: PP could be higher than what calculated up to now, at least in RSR where the ELF-calibrated SeaWiFS Chl-a bio-optical algorithm has been tuned and is likely to be more reliable than the standard SeaWiFS Chl-a bio-optical algorithm, adjusted in the world's ocean. The difference between the two values of PP is due in nearly equal parts to bio-optical algorithm and productivity model. Table 2 indicates also that the percent difference of PP in RSS and RSR is smaller according to the new calculation, but this last result should be taken cautiously as explained above.

Table 2. Temporal averaging of PP in RSR and RSS during the 16th Italian Antarctic Oceanographic Campaign according to new and standard calculations and their difference.

| PP [gC m$^{-2}$ d$^{-1}$] | | | | Difference | |
|---|---|---|---|---|---|
| D'-model applied to ELF-calibrated Chl-a | | BF-model applied to standard Chl-a | | | |
| RSR | RSS | RSR | RSS | RSR | RSS |
| 1.155 | 0.447 | 0.927 | 0.236 | 20% | 47% |

The maps of PP according to the two calculations and of their percent difference are shown in Fig. 5 for RSR. The PP values are similar in the algal blooms: their discrepancy is high only in oligotrophic waters.

Finally, we used the ELF-calibrated SeaWiFS Chl-a bio-optical algorithm and the D'-model for a new estimate of the PP in RSR and RSS in the Austral summers from the launch of OrbView-2 in 1997 (Fig. 6). For this purpose we used monthly products.

The behaviour of PP in RSS is quite regular. The variation is rather smooth and the maximum is reached in December (about 0.5 gC $m^{-2}$ $d^{-1}$). On the contrary, in RSR the maximum can be attained before or after December and the variation can be more unequal. Moreover, the values are fairly different from one year to the other.

In order to observe yearly trends, the average PP in the above mentioned Austral summers have been evaluated (Fig. 7). It is confirmed that 2001-2002 and 2002-2003 are the more and the less productive periods. The average PPs of RSR and RSS during an Austral summer are about 1 and 0.4 gC $m^{-2}$ $d^{-1}$, respectively. These values compare well with literature data [13].

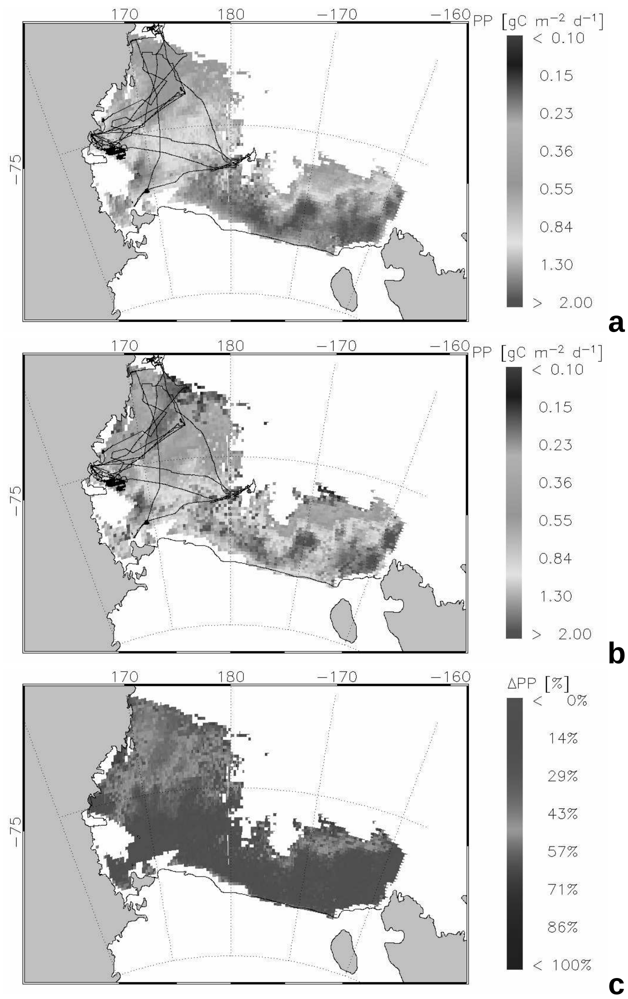


Fig. 5. Average PP in RSR, based on the monthly products of January and February 2001, calculated with: a) the ELF-calibrated SeaWiFS Chl-a bio-optical algorithm and the D'-model; b) the standard SeaWiFS Chl-a bio-optical algorithm and the BF-model. c) Percent difference between the values shown in a) and b).

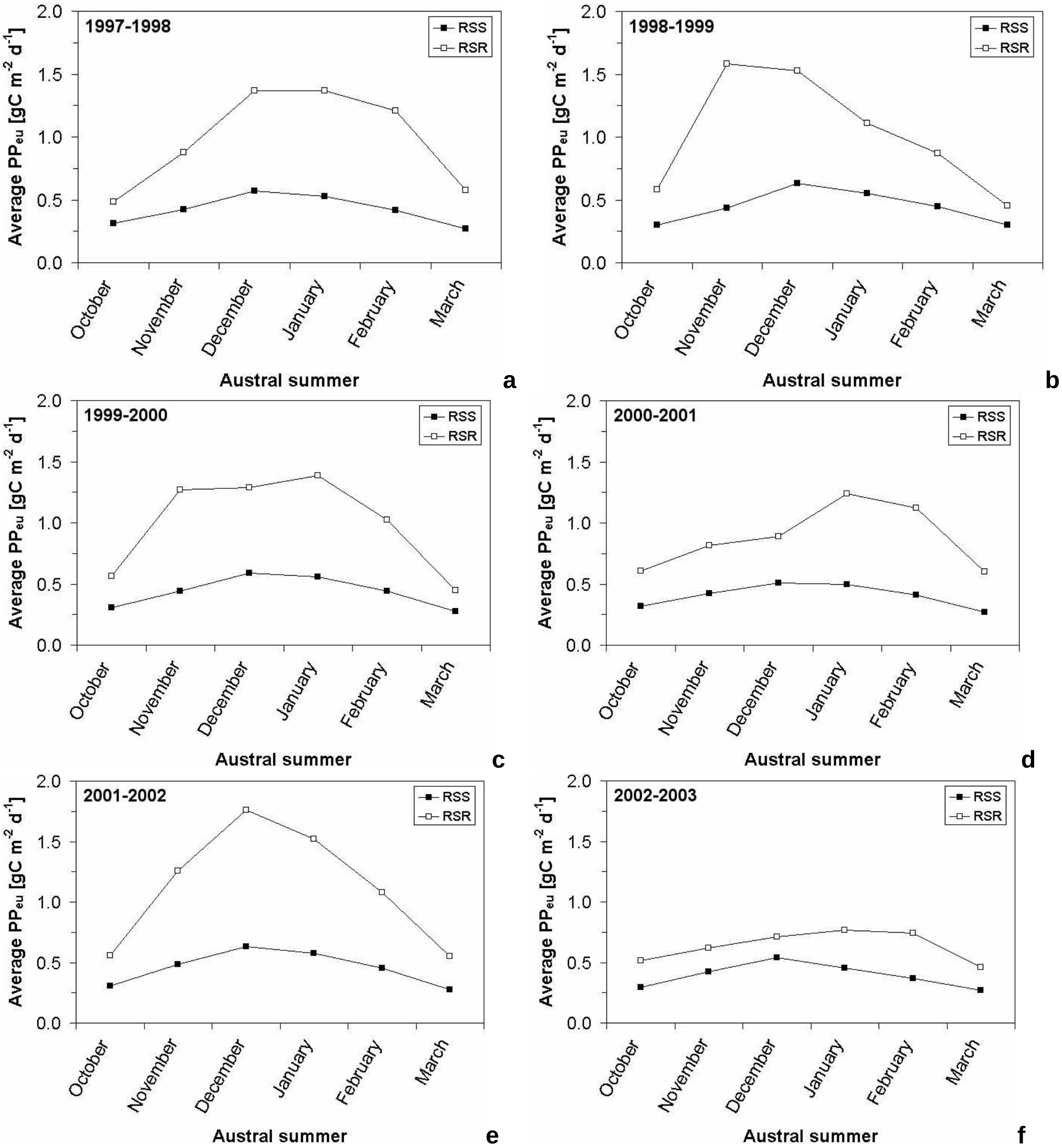


Fig. 6. Average PP calculated with the ELF-calibrated SeaWiFS Chl-a bio-optical algorithm and the D'-model in RSR and RSS during the Austral summer: a) 1997-1998; b) 1998-1999; c) 1999-2000; d) 2000-2001; e) 2001-2002; f) 2002-2003.

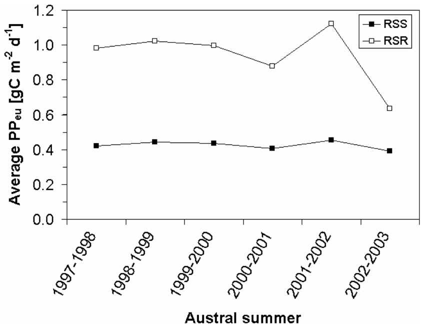


Fig. 7. Average PP calculated with the ELF-calibrated SeaWiFS Chl-a bio-optical algorithm and the D'-model in RSR and RSS from the Austral summer 1997-1998 to the Austral summer 2002-2003.

## 4. Conclusions and perspectives

In this paper a partially new PP model for the Ross Sea has been proposed: an existing PP model tuned for Antarctic coastal waters has been applied to the surface Chl-a concentrations obtained with an original bio-optical algorithm, the ELF-calibrated SeaWiFS bio-optical algorithm.

Moreover, the relative fraction of potential photosynthesis lost within the euphotic zone due to light limitation has been recalculated with the PAR measurements performed by ELF.

Our results indicate that usual PP models applied to standard surface Chl-a concentrations could underestimate PP in the Ross Sea (20% in average). The PP has been calculated monthly and yearly with the new model. The PP obtained here compare well with the values found by other authors.

This study shows that the data fusion between active and passive remote sensing, performed by ship borne lidars and satellite borne radiometers, respectively, considerably enlarge the set of simultaneous measurements useful for the accurate calibration of Chl-a algorithms and PP models. As a consequence, a consistent record of more precise PP values has been obtained, improving our picture of the biogeochemical processes affecting the Southern Ocean.

It is desirable that, with the contribution of the new satellite radiometers Moderate Resolution Imaging Spectroradiometer (MODIS) [22] and Medium Resolution Imaging Spectrometer (MERIS) [23], they become the beginning of a long term time series [24] necessary to assess the coupled ocean-atmosphere general circulation models that will help the progression of climate science from description to prediction.

### Acknowledgements

We are deeply indebted to S. Fonda Umani et al., V. Saggiomo et al. and G. Spezie et al. for kindly providing unpublished data.

This work has been supported by PNRA – Technology Sector, 5b1 and 11-5 Projects, PRNA – Oceanographic Sector, 8.3 Project and by an ENEA fellowship (Igor G. Okladnikov).

The authors would like to thank the SeaWiFS Project (Code 970.2) and the Distributed Active Archive Center (Code 902) at the Goddard Space Flight Center, Greenbelt, MD 20771, for the production and distribution of these data, respectively. These activities are sponsored by NASA's Mission to Planet Earth Program.

## References

[1] P. G. Falkowski, R. J. Scholes, E. Boyle, J. Canadell, D. Canfield, J. Elser, N. Gruber, K. Hibbard, P. Högberg, S. Linder, F. T. Mackenzie, B. Moore III, T. Pedersen, Y. Rosenthal, S. Seitzinger, V. Smetacek, W. Steffen, The global carbon cycle: a test of our knowledge of Earth as a system. Science **290**, 291-296 (2000).

[2] A. P. Cracknell, S. K. Newcombe, A. F. Black, N. E. Kirby, The ABDMAP (Algal Bloom Detection, Monitoring and Prediction) concerted action. International Journal of Remote Sensing **22**, 205-247 (2001).

[3] R. Reuter, D. Diebel, T. Hengstermann, Oceanographic laser remote sensing: measurement of hydrographic fronts in the German Bight and in the Northern Adriatic Sea, International Journal of Remote Sensing **14**, 823-848 (1993).

[4] L. Fiorani, S. Mattei, S. Vetrella, Laser methods for the atmospheric correction of marine radiance data sensed from satellite. Proceedings of SPIE, **3496**, 176-187 (1998).

[5] J. E. O'Reilly, S. Maritorena, M. C. O'Brien, D. A. Siegel, D. Toole, D. Menzies, R. C. Smith, J. L. Mueller, B. Greg Mitchell, M. Kahru, F. P. Chavez, P. Strutton, G. F. Cota, S. B. Hooker, C. R. McClain, K. L. Carder, F. Müller-Karger, L. Harding, A. Magnuson, D. Phinney, G. F. Moore, J. Aiken, K. R. Arrigo, R. Letelier, M. Culver, SeaWiFS Postlaunch Calibration and Validation Analyses, Part 3. NASA Technical Memorandum 2000-206892, Volume 11, Eds. S. B. Hooker and E. R. Firestone, NASA, Greenbelt, US (2000).

[6] J. E. O'Reilly, S. Maritorena, B. G. Mitchell, D. A. Siegel, K. L. Carder, S. A. Garver, M. Kahru, C. McClain, Ocean color chlorophyll algorithms for SeaWiFS. Journal of Geophysical Research C, **103**, 24937-24953 (1998).
[7] P. W. Boyd, Environmental factors controlling phytoplankton processes in the Southern Ocean. Journal of Phycology, **38**, 844-861 (2002).
[8] R. Barbini, F. Colao, A. Palucci, S. Ribezzo, T. Hermsen, S. Orlando, Atmospheric Water Vapor Measurements with the ENEA Lidar Station. ENEA Technical Report RT/INN/90/53, ENEA, Rome, Italy (1990).
[9] R. Barbini, F. Colao, R. Fantoni, L. Fiorani, A. Palucci, Remote sensing of the Southern Ocean: techniques and results, J. Optoelectron. Adv. Mater. **3**, 817-830 (2001).
[10] S. B. Hooker, W. E. Esaias, G. C. Feldman, W. W. Gregg, C. R. McClain, An overview of SeaWiFS and ocean color. SeaWiFS Technical Report Series, NASA Technical Memorandum 104566, Vol. **1**, Eds. S. B. Hooker and E. R. Firestone, NASA, Greenbelt, US (1992).
[11] R. Barbini, F. Colao, R. Fantoni, L. Fiorani, A. Palucci, Lidar fluorosensor calibration of the SeaWiFS chlorophyll algorithm in the Ross Sea, International Journal of Remote Sensing **24**, 3205-3218 (2003).
[12] C. R. McClain, G. C. Feldman, S. B. Hooker, An overview of the SeaWiFS project and strategies for producing a climate research quality global ocean bio-optical time series. Deep-Sea Research II, **51**, 5-42 (2004).
[13] K. R. Arrigo, D. L. Worthen, A. Schnell, M. P. Lizotte, Primary production in Southern Ocean waters, Journal of Geophysical Research C, **103**, 15587-15600 (1998).
[14] M. J. Behrenfeld, P. G. Falkowski, A consumer's guide to phytoplankton primary productivity models. Limnology and Oceanography **42**, 1479-1491 (1997).
[15] P. G. Falkowski, M. J. Behrenfeld, W. E. Esaias, W. Balch, J. W. Campbell, R. L. Iverson, D. A. Kiefer, A. Morel, J. A. Yoder, Satellite primary productivity data and algorithm development: a science plan for Mission to the Planet Earth. SeaWiFS Technical Report Series, NASA Technical Memorandum 104566, Vol. **42**, Eds. S. B. Hooker and E. R. Firestone, NASA, Greenbelt, US (1998).
[16] M. J. Behrenfeld, P. G. Falkowski, Photosynthetic rates derived from satellite-based chlorophyll concentrations. Limnology and Oceanography **42**, 1-20 (1997).
[17] H. M. Dierssen, M. Vernet, R. C. Smith, Optimizing models for remotely estimating primary production in Antarctic coastal waters. Antarctic Science, **12**, 20-32 (2000).
[18] R. C. Smith, K. S. Baker, H. M. Dierssen, S. E. Stammerjohn, M. Vernet, Bio-optical modeling of primary production from SeaWiFS ocean color data for the western Antarctic Peninsula region, E-proceedings of Ocean Optics XV, Eds. S. Ackleson and J. Marra, Musée Océanographique, Monaco, Monaco (2000).
[19] A. Morel, J.-F. Berthon, Surface pigments, algal biomass profiles, and potential production of the euphotic layer: relationships reinvestigated in view of remote-sensing applications. Limnology and Oceanography **34**, 1545-1562 (1989).
[20] W. D. Sellers, Physical Climatology, University of Chicago Press, Chicago, US (1965).
[21] WOCE Data Products Committee, WOCE global data: satellite data, version 3.0, WOCE Report 180/02, WOCE International Project Office, Southampton, UK (2002).
[22] W. E. Esaias, M. R. Abbott, I. Barton, O. B. Brown, J. W. Campbell, K. L. Carder, D. K. Clark, R. H. Evans, F. E. Hoge, H. R. Gordon, W. M. Balch, R. Letelier, P. J. Minnett, An overview of MODIS capabilities for ocean science observations. IEEE Transactions on Geoscience and Remote Sensing, **36**, 1250-1265 (1998).
[23] J.-P. Huot, H. Tait, M. Rast, S. Delwart, J.-L. Bézy, G. Levrini, The optical imaging instruments and their applications: AATSR and MERIS. ESA Bulletin, **106**, 56-66 (2002).
[24] R. Barbini, F. Colao, L. De Dominicis, R. Fantoni, L. Fiorani, A. Palucci, E. S. Artamonov, Analysis of simultaneous chlorophyll measurements by lidar fluorosensor, MODIS and SeaWiFS, International Journal of Remote Sensing, **25**, 2095-2110 (2004).